Can undersea voltage measurements detect tsunamis?

C. Manoj[1,2,5], A. Kuvshinov[3,6], S. Neetu[4], and T. Harinarayana[5]

[1]Cooperative Institute for Research in Environmental Sciences, University of Colorado, Boulder, Colorado, USA
[2]NGDC/NOAA E/CG2, 325 Broadway, Boulder, CO80305, USA
[3]Institute of Geophysics, ETH-Zurich, Zurich, Switzerland
[4]National Institute of Oceanography, Goa, India
[5]National Geophysical Research Institute, Hyderabad 500007, India
[6]Institute of Terrestrial Magnetism, Ionosphere and Radiowave Propagation, Russian Academy of Sciences, 142190, Troitsk, Moscow region, Russia

(Received September 16, 2008; Revised August 17, 2009; Accepted October 7, 2009; Online published March 4, 2010)

The movement of electrically conducting ocean water in the ambient geomagnetic field induces secondary electric and magnetic fields in the oceans. Ocean water transport is now routinely inferred from undersea cable voltage data. We try to answer the question whether the method could also be useful to detect tsunami. A barotropic shallow water model along with a three-dimensional electromagnetic induction code was used to predict the electric fields induced by the Indian Ocean Tsunami occurred on December 26, 2004. We show that the ocean flow related to the Indian Ocean Tsunami must have induced electric voltages of the order of $\pm$500 mV across the existing submarine cables in the Indian Ocean. The electric fields induced by the Tsunami flow have strength within the range of $\pm$10 mV/km, with enhancements along the main flow region and near the coasts and islands. Thus, making use of the in-service or retired submarine cables to measure the electric potential across oceans, it may be possible to detect water movement related to tsunami.
Key words: Tsunami, motional induction, Indian Ocean, electric field, submarine cables.

1. Introduction

The largest earthquake of the past 40 years (seismic moment magnitude (M_w) was in the range from 9.1 to 9.3) in the Indian Ocean on December 26, 2004 resulted in a devastating Tsunami, which killed more that 280,000 people in the south-east Asian region (Lay *et al.*, 2005). Though tide gauge measurements can be used to measure the tsunami waves along the coast, the detection and monitoring of tsunami generated waves in the open ocean is challenging. The reason is that the spatial scale of tsunami waves is large (larger than 100 km), and the vertical surface displacement is very small (smaller than few cm) in the open ocean (Artru *et al.*, 2005). The tsunami related ocean flow can be described as barotropic, non-dispersive surface gravity wave. Though the particle motions in the water associated with such waves have speed less than few centimeters per second, they affect the entire water column.

Motional induction is sensitive to the movement of the entire water column (Flosadóttir *et al.*, 1997) and offer an alternative way of monitoring ocean flow. Secondary electric and magnetic fields are induced when electrically conductive ocean water moves across the ambient geomagnetic field (Sanford, 1971). The renewed interest in this technique is primarily due to advances in high precision measurements of electric and magnetic fields and sophisticated numerical simulations available now. Using a forward simulation, Tyler (2005) demonstrated that the magnetic fields generated by the Indian ocean tsunami could have reached an amplitude of 4 nT. He proposed that the magnetic signal could possibly be detected in advance and the method may be useful in future tsunami monitoring systems. However, no reported attempt has been made to study the electric fields in the oceans due to tsunami flow.

Larsen and Sanford (1985) proposed that the water transport across the Florida Strait can be estimated in a precise manner by measuring the cross-stream voltage using a submarine cable. Subsequently, the water transport estimates are regularly carried out across Florida Strait using undersea voltage measurements (Baringer and Larsen, 2001). Linear relationship between the submarine voltage data and the water transport was also reported by Kim *et al.* (2004) and Nilsson *et al.* (2007). Flosadóttir *et al.* (1997) show that the relationship between voltage and cross-cable transport fluctuations can be remarkably linear over long distances. Thomson *et al.* (1995) report voltage variations across an undersea cable that have time associations with the tsunami produced by the Cape Mendocino earthquake of 1992. They obtained enhanced voltage power spectra, for the interval following the main shock as compared to a 10-day average. Indian Ocean has a network of undersea cables for telecommunication purposes (TeleGeography, 2007). Many of these cable systems are made of optical fibers. However, Sigray *et al.* (2004), Medford *et al.* (1989) and Flosadóttir *et al.* (1997) discuss various methods to measure voltage across an undersea optical cable system. It would, thus be

doi:10.5047/eps.2009.10.001

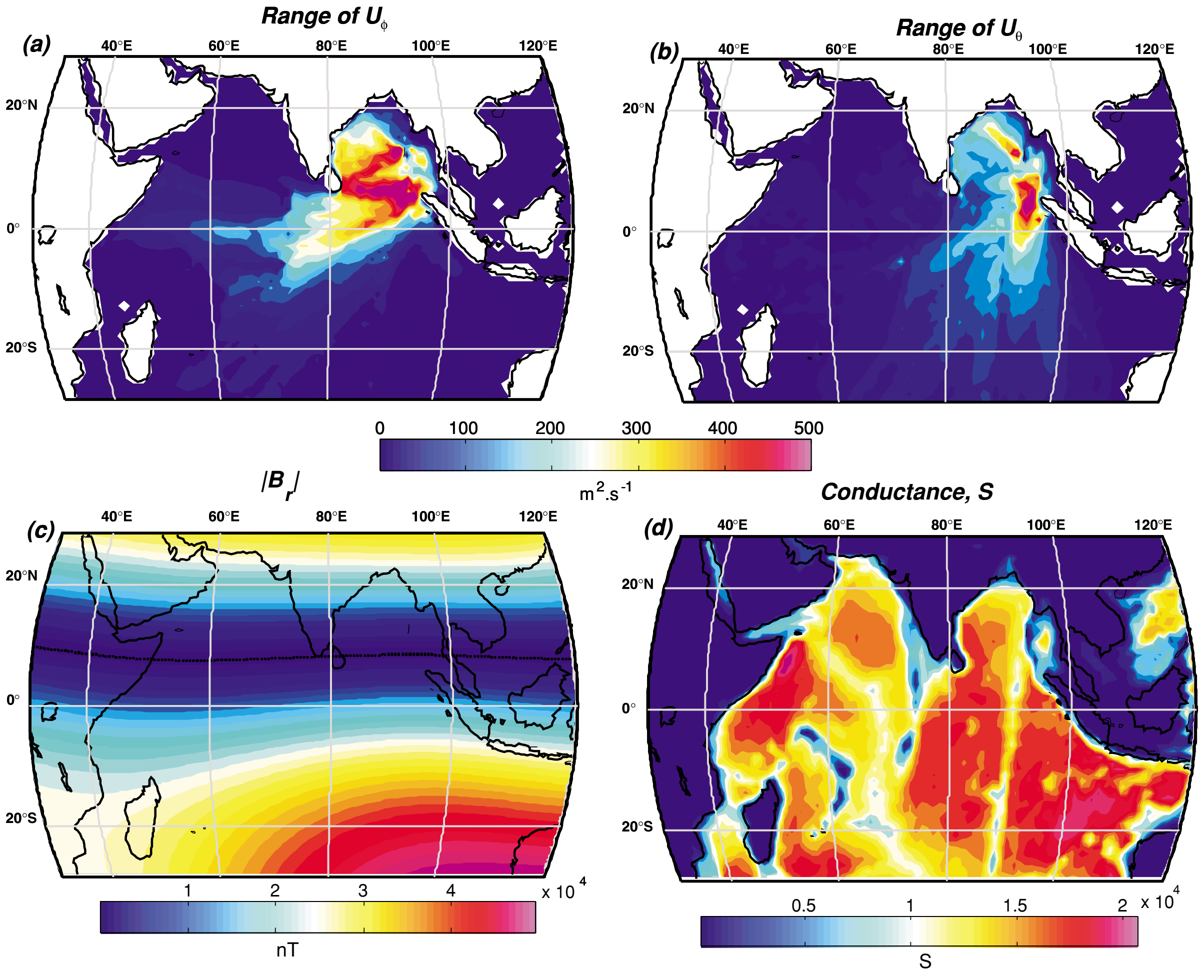

Fig. 1. The input parameters for the modeling. Top panels show the range of Eastward (U_φ—a) and Southward (U_ϑ—b) components of the vertically integrated horizontal flow velocities (m^2 s^{-1}). (c) The radial component of the geomagnetic main field $|B_r^m|$ (nT). The dotted line indicates the geomagnetic dip-equator (d) Shell conductance (S).

interesting to predict the voltage variations across the network of cables in Indian Ocean due to the motional induction by tsunami.

In this paper we address two important questions regarding motional induction by tsunamis: 1) What are the amplitude and spatial distribution of the induced electric fields in the oceans? 2) Can undersea cable voltage measurements possibly detect the temporal variations of these electric fields? To answer these questions, we use a barotropic tsunami model and a state-of-the-art 3-D EM induction code to simulate the electric and magnetic fields generated by the Indian Ocean Tsunami. We will first describe the tsunami model, followed by the numerical simulations, and finally discuss the results of the simulation.

2. Numerical Simulation

We use a barotropic model (Unnikrishnan *et al.*, 1999; Sindhu *et al.*, 2007) based on the shallow water equations to simulate the 26 December 2004 Tsunami propagation in the region. The model is run on 5 arc minute spatial grid resolution using ETOPO5 (www.ngdc.noaa.gov) bathymetry. The time step for the computation was chosen as 10 seconds to satisfy a stability condition. We use the tsunami source region and the vertical sea surface displacement estimated by Hirata *et al.* (2006) as the initial condition for the model. The model output (vertically integrated transport) is generated for every $1^\circ \times 1^\circ$ cell and for every minute for a duration of 10 hours from the onset of the tsunami.

To predict the electric fields due to the tsunami wave motion, we adopt the integral equation numerical solution described by Kuvshinov *et al.* (2002) and Kuvshinov and Olsen (2005). The solution allows for simulating electromagnetic (EM) field in a spherical models of the Earth with three-dimensional (3-D) distribution of electrical conductivity. These models consist of a number of 3-D conductivity anomalies, embedded in a host radially symmetric (1-D) section of conductivity $\sigma_b(r)$; here r is the distance from the Earth's centre. Within this approach Maxwell's equations in the frequency domain,

$$\begin{aligned} \nabla \times \mathbf{H} &= \sigma \mathbf{E} + \mathbf{j}^{\text{ext}}, \\ \nabla \times \mathbf{E} &= i\omega\mu_o \mathbf{H}, \end{aligned} \tag{1}$$

are reduced, in accordance with the modified iterative-dissipative method (Singer, 1995), to a scattering equation of specific type (cf. Pankratov *et al.*, 1997). Here, $\mathbf{j}^{\text{ext}}$ is the extraneous (impressed) current, time-harmonic dependency is $e^{-i\omega t}$, μ_o is the magnetic permeability of free space,

$i = \sqrt{-1}$, $\omega = 2\pi/T$ is the angular frequency, T is the period of the variations, $\sigma(r, \vartheta, \varphi)$ is the conductivity distribution in the model, and ϑ and φ are co-latitude and longitude respectively. Once the scattering equation is solved (and thus the electric field at depths occupied by 3-D anomalies is determined), the electric field $\mathbf{E}$ at the observation points $\mathbf{r} \in V^{\mathrm{obs}}$ is calculated as,

$$\mathbf{E}(\mathbf{r}) = \int_{V^{\mathrm{ext}}} G_b^e(\mathbf{r}, \mathbf{r}')\mathbf{j}^{\mathrm{ext}}(\mathbf{r}')dv' + \int_{V^{\mathrm{mod}}} G_b^e(\mathbf{r}, \mathbf{r}')\mathbf{j}^q(\mathbf{r}')dv', \qquad (2)$$

where $\mathbf{j}^q = (\sigma - \sigma_b)\mathbf{E}$, G_b^e is the Green's tensor for the radially symmetric conductor $\sigma_b(r)$, $\mathbf{r} = (r, \vartheta, \varphi)$, $\mathbf{r}' = (r', \vartheta', \varphi')$, V^{ext} and V^{mod} are the spherical layers where impressed current $\mathbf{j}^{\mathrm{ext}}$ and 3-D conductivity anomalies are present.

For our case, the 3-D model simplifies to a surface spherical shell of conductance $S(\vartheta, \varphi)$, underlain by a 1-D conductor. Then, $\mathbf{j}^{\mathrm{ext}}$ reduces to the sheet current density $\mathbf{J}_\tau^{\mathrm{ext}}$, which is calculated as,

$$\mathbf{J}_\tau^{\mathrm{ext}} = \sigma_w \left(\mathbf{U} \times \mathbf{e}_r B_r^m\right), \qquad (3)$$

where σ_w is the mean conductivity of sea-water (3.2 S/m), $\mathbf{U}$ are the depth-integrated velocities derived from the tsunami model, $\mathbf{e}_r$ is the outward unit vector and B_r^m is the radial component of the geomagnetic main field as derived from POMME model (Maus *et al.*, 2006).

A realistic model of the shell conductance $S(\vartheta, \varphi)$ on a grid $1^\circ \times 1^\circ$ is obtained by considering the contributions from sea-water and sediments (Manoj *et al.*, 2006). The 1-D conductivity model is compiled from the four-layer model of Schmucker (1985) for depth greater than 100 km (0.014 S/m between 100 and 500 km, 0.062 S/m between 500 and 750 km, and 2.4 S/m at depths greater than 750 km) whereas for the upper 100 km, we assume $3{\cdot}10^{-4}$ S/m.

Figure 1 shows the spatial distribution of the input data sets used. The top panels show the range of the Eastward (U_φ—a) and Southward (U_ϑ—b) components of the depth-integrated velocities. We plot the differences between the maximum and minimum values of velocities at each grid point during the entire period of simulation. The tsunami-flow is intense in the northern Indian Ocean. The radial component of the geomagnetic main field, B_r^m (Fig. 1(c)) has a narrow band of small amplitude along the geomagnetic dip-equator (marked with dashed line). The conductance map for the region (Fig. 1(d)) is dominated by the effect of the ocean topography. Electrical conductance of ocean is significantly higher than that of continental upper crust.

The tsunami-flow data at centers of the cell were converted to frequency domain. The numerical simulations were performed independently for each frequency. Finally an inverse Fourier transform of the results gives the time series signals at each grid points.

3. Results

We plot the maps of the maximum range of the horizontal electric field in the ocean induced by the tsunami during the entire period of simulation in Figs. 2(a) and (b). The electric fields have strength within the range ±10 mV/km, with strong signals along the main flow region and near the coasts and islands. The enhancement of the electric field along the ocean-continent boundary is due to the large lateral electrical conductivity contrast (cf. Kuvshinov *et al.*, 2006) at ocean-land boundaries. In the open ocean, the strength of the electric field is within ±2 mV/km. The spatial distribution of the electric field is controlled by the flow velocities and the radial component of the geomagnetic main field B_r^m (see Eq. (1)). A band of low signal strength along 10°N latitude, in the NE Indian Ocean, is due to the weak geomagnetic radial component along the dip-equator (Fig. 1(c)). The Mascarene ridge system, along the southern part of the 60°E longitude (Fig. 1(d)), dampens the tsunami-flow and results in weak electric fields around Madagascar.

To calculate the voltage difference, we select the paths along three in-service cables in Indian Ocean, viz. SAFE, SEA-ME-WE3 and TATA (Fig. 2(a)). The locations of the submarine cables are obtained from TeleGeography (2007). We predict the voltage variations between the cable landing locations marked A to E, in three combinations. The first combination, A–B (Reunion Island to Penang, distance 5716 km) is the longest among all. The other landing pairs are C–D (Cochin, India–Singapore, distance 3180 km) and E–D (Chennai, India–Singapore, distance 2902 km). The voltage across the landings was calculated by integrating the electric field between them for the entire simulation period of 10 hours with time step 1 minute.

The propagation of the electric field along the cable A–B as a function of time and distance is shown with the X-T diagram (Fig. 2(c)). The black line indicates the time of the first arrival of the tsunami waves along the cable. Near the rupture zone, the arrival time is not accurately defined and is shown with dashed lines. The larger fluctuations of the electric feld signal coincides with the arrival of the leading tsunami waves.

Figure 2(d) shows the simulated voltage time series across the three selected cable landing pairs. The voltages across the undersea cables have amplitudes in the range ±500 mV. The largest signals are predicted across A–B, which is also the longest among the three. This cable mostly runs parallel to the direction of the main wave motion. Both C–D and E–D lines run parallel to the geomagnetic dip-equator and hence the amplitudes of voltage variation across them are lower than that of A–B. The time series represent the continuous variation of the electric fields integrated between two end points of the cable. The predominant period of the voltage variation is approximately 20 minutes. The voltage variation inherits this periodicity from the tsunami model we use. Titov *et al.* (2005) reports periodicities in the range of 15–60 minutes for the Indian Ocean Tsunami.

We also examine the linearity of the relationship between the voltage across the cable and the movement of water perpendicular to the cable. Figure 3 shows the model voltage data plotted against the water transport across cable A–B. The linearity of their relationship indicates that relative water transport fluctuations corresponds to the relative voltage fluctuations across the cable. Here, 1 Sv (1 Sv $\equiv 10^6$ m^3 s^{-1}) of water transport results in approximately

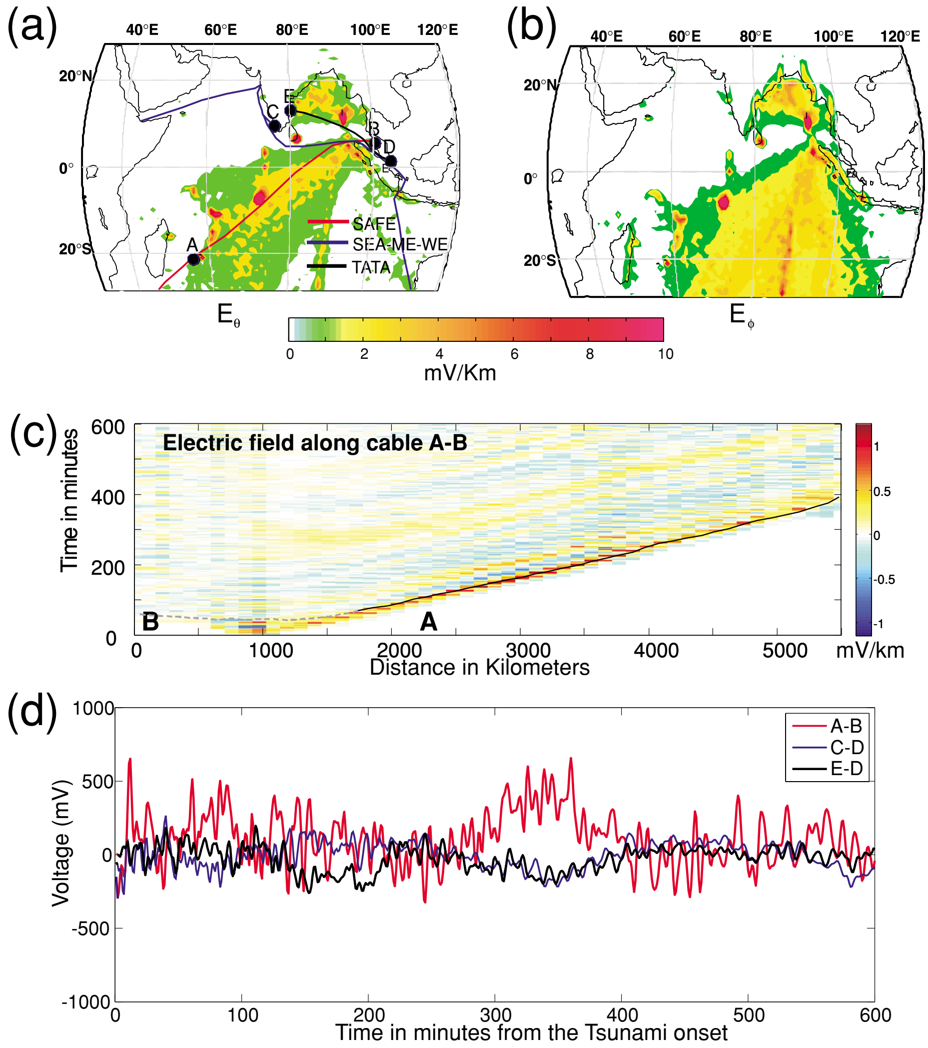

Fig. 2. Results. (a) The range of Southward (E_ϑ) component. (b) The range of Eastward (E_φ) component. The colored lines show the network of undersea communication cables in the Indian Ocean region. (c) X-T diagram showing the propagation of the induced electric field along the cable A–B. The black line indicates the time of the first arrival of the tsunami waves along the cable. (d) The simulated time series of the voltages across the three undersea cables.

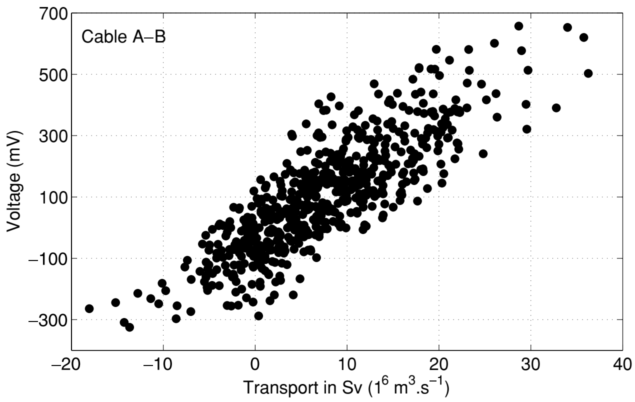

Fig. 3. Plot of the model voltage against the water transport across cable A–B during the simulation period. For this cable, 1 Sv of water transport induces approximately 18 mV of voltage across the cable.

18 mV of voltage across the cable. As the relationship between flow and voltage is also influenced by the location of the flow relative to the topography, electrical conductivity of ocean sediments and the Earth's magnetic field, the slope parameter can change from place to place.

4. Discussion and Conclusion

Lilley *et al.* (1986) and Meinen *et al.* (2002) discuss the use of sea-floor electric field measurements to monitor the water flow. The measurement of electric fields on sea floor with an array of "electrometers" (for example the SAFDE project (Luther *et al.*, 1997)) around tectonically active zones may be able to detect the changes in electric field due to a tsunami. However, "electrometers" need to be deployed in a favorable location, with sufficient spatial density, to detect tsunamis.

We find that the voltage variation across the stations reaches up to ±500 mV, which is clearly a measurable signal (cf. Fujii and Utada, 2000). Larsen (1991) gives an estimate of 30 mV of error base for submarine cable voltage measurements across Florida Strait. It is worth to exploit the existing and retired submarine cable system to detect the voltage variations in places like northern Indian Ocean, where several tectonically active faults systems exist. A cable across a tectonically active ocean floor/subduction zone may be able to detect the tsunami-flows in a large area of ocean. Though this work focuses on one large tsunami event in the Indian Ocean, the results are important to other parts of the world as well. Especially, the effect of motional induction can be more prominent in higher latitudes due to increased amplitudes of the radial component of the geomagnetic main field (Tyler, 2005, Fig. 1). The existing undersea measurement system, for example in the North Pacific Ocean (Fujii and Utada, 2000; Utada *et al.*, 2003) may be used to detect the tsunami induced voltage variations.

It is relevant to mention that other than the work by Thomson *et al.* (1995), there is no reported measurement of tsunami induced electric fields. Another complication is the extraction of the electric signals due to tsunami flow from the measured cable data. The biases in the voltages caused by electrochemical processes at cable-ocean contact (Flosadóttir *et al.*, 1997) can add noise to the measured data. In addition, the electric fields due to external (ionospheric and magnetospheric) sources or/and motional induction from other types of ocean flow (say, ocean circulation and tides) can also be present in the cable data (Larsen, 1980, 1992).

However, the instabilities in the cable-ocean contacts can be minimized by proper selection of contact locations and high-quality electrodes (Filloux, 1987). An accuracy of 1 mV is readily achievable with the use of proper electrodes at the cable-ocean contacts (Larsen, 1991; Filloux, 1987). The tidal variation can be estimated and removed by the sophisticated numerical schemes presently available (Tyler, 2005; Kuvshinov *et al.*, 2006). Typical periodicities associated with tsunami-related voltage variations make it possible to separate them from the background noise by comparing with geomagnetic data that are not influenced by motional induction. The method discussed by Larsen (1997) may be adopted for this purpose. However, the external signals may persist in the cable data in the absence of data from nearby magnetic reference stations.

Array of bottom pressure sensors with reliable telemetry system are used to detect water movement in modern tsunami-monitoring systems (González *et al.*, 1998). We show that undersea voltage measurements can also detect water movement. A drawback of voltage measurements in this context will be lack of the location information of water movement along the cable. This shortcoming can be overcome if a network of submarine cables is available in the area. Another possibility is to first locate the earthquake epicenter and then analyze the voltage data along the cables near that location. Considering that submarine cables are available in almost all the oceans (TeleGeography, 2007) and the low-cost of voltage measurements across them, their use may be explored for oceans where *in situ* measurements of bottom pressure is absent or sparse.

5. Summary

Using shallow water, barotropic tsunami model, along with a 3-D EM simulation code, we computed the electric fields induced by the Dec. 26 Indian Ocean Tsunami. The electric fields have strength within the range of ± 10 mV/km, with enhancements along the main flow region and near the coasts and islands. Tsunami must have induced electric voltages of the order of ± 500 mV across the existing submarine cables in the Indian Ocean. Thus, making use of the in-service or retired submarine cables to measure the electric potential across oceans, it may be possible to detect water movement related to tsunami.

Acknowledgments. Suggestions by Stefan Maus and Joy Ikelman have improved an earlier version of this paper. AK acknowledges the support of the Russian Foundation for Basic Research to this work through grant No. 09-05-01071-a. R. N. Singh (NGRI) helped to select a suitable tsunami model. This is NIO contribution 4631. We thank Robert Tyler and an anonymous reviewer for their comments on this paper.

References

Artru, J., V. Ducic, H. Kanamori, P. Lognonné, and M. Murakami, Ionospheric detection of gravity waves induced by tsunamis, *Geophys. J. Int.*, **160**, 840–848, 10.1111/j.1365-246X.2005.02552.x, 2005.

Baringer, M. O. and J. C. Larsen, Sixteen years of Florida Current transport at 27° N, *Geophys. Res. Lett.*, 28, 3179–3182, 10.1029/2001GL013246, 2001.

Filloux, J. H., Instrumentation and experimental methods for oceanic studies, in *Geomagnetism*, edited by Jacobs, J., 143–248, Academic Press, 1987.

Flosadóttir, Á. H., J. C. Larsen, and J. T. Smith, The relation of seafloor voltages to ocean transports in North Atlantic circulation models: Model results and practical considerations for transport monitoring, *J. Phys. Oceanogr*, **27**, 1547–1565, 1997.

Fujii, I. and H. Utada, On geoelectric potential variations over a planetary scale, *Memoirs of the Kakioka Magnetic Observatory*, **29**, 1–81, 2000.

González, F. I., H. M. Milburn, E. N. Bernard, and J. Newman, Deep-ocean assessment and reporting of tsunamis (DART): Brief overview and status report, *Proceedings of the International Workshop on Tsunami Disaster Mitigation. Tokyo, Japan*, 118–129, 1998.

Hirata, K., K. Satake, Y. Tanioka, T. Kuragano, Y. Hasegawa, Y. Hayashi, and N. Hamada, The 2004 Indian Ocean tsunami: Tsunami source model from satellite altimetry, *Earth Planets Space*, **58**(2), 195–201, 2006.

Kim, K., S. J. Lyu, Y. G. Kim, B. H. Choi, K. Taira, H. T. Perkins, W. J. Teague, and J. W. Book, Monitoring volume transport through measurement of cable voltage across the Korea Strait, *J. Atmos. Oceanic Technol.*, **21**, 671–682, 2004.

Kuvshinov, A. and N. Olsen, 3-D Modelling of the magnetic fields due to ocean tidal flow, in *Earth Observation With CHAMP: Results From Three Years in Orbit*, edited by Reigber, C., H. Lühr, P. Schwintzer, and J. Wickert, 359–365, Springer, Berlin-Heidelberg, 10.1007/3-540-26800-6_57, 2005.

Kuvshinov, A. V., D. B. Avdeev, O. V. Pankratov, S. A. Golyshev, and N. Olsen, Modelling electromagnetic fields in 3D spherical Earth using fast integral equation approach, in *3D Electromagnetics*, edited by Zhdanov, M. S. and P. E. Wannamaker, 43–54, Elsevier, Holland, 2002.

Kuvshinov, A., A. Junge, and H. Utada, 3-D modelling the electric field due to ocean tidal flow and comparison with observations, *Geophys. Res. Lett.*, **33**, 6314, 10.1029/2005GL025043, 2006.

Larsen, J. C., Electromagnetic response functions from interrupted and noisy data, *J. Geomag. Geoelectr.*, **32**, 89–103, 1980.

Larsen, J. C., Transport measurements from in-service undersea telephone cables, *IEEE J. Oce. Engg.*, **16**(4), 313–318, 1991.

Larsen, J. C., Transport and heat flux of the Florida current at 27 degrees N derived from cross-stream voltages and profiling data: Theory and observations, *Philos. Trans. R. Soc. A, Phys. Sci. Eng.*, **338**(1650), 169–236, 1992.

Larsen, J. C., Noise reduction in electromagnetic time series to improve detection of seismic-induced signals, *J. Geomag. Geoelectr.*, **49**(11–12), 1257–1265, 1997.

Larsen, J. C. and T. B. Sanford, Florida current volume transports from voltage measurements, *Science*, **227**, 302–304, 1985.

Lay, T., H. Kanamori, C. J. Ammon, M. Nettles, S. N. Ward, R. C. Aster, S. L. Beck, S. L. Bilek, M. R. Brudzinski, R. Butler, H. R. DeShon, G. Ekström, K. Satake, and S. Sipkin, The great Sumatra-Andaman earthquake of 26 December 2004, *Science*, **308**, 1127–1133, 10.1126/science.1112250, 2005.

Lilley, F. E. M., J. H. Filloux, N. L. Bindoff, I. J. Ferguson, and P. J. Mulhearn, Barotropic flow of a warm-core ring from seafloor electric measurements, *J. Geophys. Res.*, **91**, 12979–12984, 1986.

Luther, D. S., A. D. Chave, J. A. Church, J. H. Filloux, J. G. Richman, S. R. Rintoul, and D. R. Watts, The Sub-Antarctic Flux and Dynamics Experiment (SAFDE), *WOCE Notes*, **9**(2), 8–12, 1997.

Manoj, C., A. Kuvshinov, S. Maus, and H. Lühr, Ocean circulation generated magnetic signals, *Earth Planets Space*, **58**, 429–439, 2006.

Maus, S., M. Rother, C. Stolle, W. Mai, S. Choi, H. Lühr, D. Cooke, and C. Roth, Third generation of the Potsdam Magnetic Model of the Earth (POMME), *Geochem. Geophys. Geosyst.*, **7**, 7008-+, 10.1029/2006GC001269, 2006.

Medford, L. V., L. J. Lanzerotti, J. S. Kraus, and C. G. Maclennan, Transatlantic earth potential variations during the March 1989 magnetic storms, *Geophys. Res. Lett.*, **16**, 1145–1148, 1989.

Meinen, C. S., D. S. Luther, D. R. Watts, K. L. Tracey, A. D. Chave, and J. Richman, Combining inverted echo sounder and horizontal electric field recorder measurements to obtain absolute velocity profiles, *J. Atmos. Oceanic Technol.*, **19**(10), 1653–1664, 2002.

Nilsson, J. A., P. Sigray, P. Sigray, and R. H. Tyler, Geo-electric monitoring of wind-driven barotropic transports in the Baltic Sea, *J. Atmos. Oceanic Technol.*, **24**(9), 1655–1664, 2007.

Pankratov, O. V., A. V. Kuvshinov, and D. B. Avdeev, High-performance three-dimensional electromagnetic modelling using modified Neumann series. Anisotropic Earth, *J. Geomag. Geoelectr.*, **49**(11–12), 1519–1539, 1997.

Sanford, T. B., Motionally induced electric and magnetic fields in the sea, *J. Geophys. Res.*, **76**, 3476–3492, 1971.

Schmucker, U., *Magnetic and electric fields due to electromagnetic induction by external sources, electrical properties of the earth interior*, Springer Verlag, Berlin, Landolt-Boernstein New Series Group, 5/2b, 1985.

Sigray, P., P. Lundberg, and K. Döös, Observations of transport variability in the Baltic Sea by parasitic use of a fiber-optic cable, *J. Atmos. Oceanic Technol.*, **21**(7), 1112–1120, 2004.

Sindhu, B., I. Suresh, A. S. Unnikrishnan, N. V. Bhatkar, S. Neetu, and G. S. Michael, Improved bathymetric datasets for the shallow water regions in the Indian Ocean, *J. Earth Syst. Sci.*, **116**(3), 261–274, 2007.

Singer, B. S., Method for solution of Maxwell's equations in non-uniform media, *Geophys. J. Int.*, **120**, 590–598, 1995.

TeleGeography, *Submarine Cable Map 2007*, Washington: TeleGeography, http://www.telegeography.com/products/map_cable/images/sub_cable_2007_large.jpg, 2007.

Thomson, D. J., L. J. Lanzerotti, C. G. Maclennan, and L. V. Medford, Ocean cable measurements of the tsunami signal from the 1992 Cape Mendocino earthquake, *Pure Appl. Geophys.*, **144**, 427–440, 10.1007/BF00874376, 1995.

Titov, V., A. B. Rabinovich, H. O. Mofjeld, R. E. Thomson, and F. I. Gonzalez, The global reach of the 26 December 2004 Sumatra tsunami, *Science*, **309**(5743), 2045–2048, 2005.

Tyler, R. H., A simple formula for estimating the magnetic fields generated by tsunami flow, *Geophys. Res. Lett.*, **32**, 9608-+, 10.1029/2005GL022429, 2005.

Unnikrishnan, A. S., S. R. Shetye, and G. S. Michael, Tidal propagation in the Gulf of Khambhat, Bombay High, and surrounding areas, *Proceedings of the Indian Academy of Sciences. Earth and Planetary Sciences*, **108**(3), 155–177, 1999.

Utada, H., T. Koyama, H. Shimizu, and A. D. Chave, A semi-global reference model for electrical conductivity in the mid-mantle beneath the north Pacific region, *Geophys. Res. Lett.*, **30**, 43-1, 2003.

C. Manoj (e-mail: manoj.c.nair@noaa.gov), A. Kuvshinov, S. Neetu, and T. Harinarayana